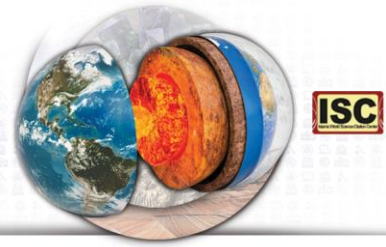# The Kinematic Association of Folds and Faults in the Zagros Hinterland Fold-and-Thrust Belts

Mohammad Ali Ghanbarian
Department of Earth Sciences, College of Sciences
Shiraz University
Shiraz, Iran
maghanbarian@shirazu.ac.ir

Reza Derakhshani
Department of Geology
Shahid Bahonar University of Kerman
Kerman, Iran.
Department of Earth Sciences
Utrecht University,
Utrecht, The Netherlands
r.derakhshani@uu.nl

Abstract— **The structural architecture and folds and faults relationships of a significant segment of the south-central part of the Zagros' hinterland are investigated in this study through stereoscopy of aerial photographs, interpretations of satellite images, consideration of the major ground topographic variations, and field research. This research found that there must have been at least two major deformation events: (1) a ductile phase, which is older than the Eocene, and (2) a semi-brittle deformation stage, which is younger than the early Miocene and is represented by thrusting, folding, and strike-slip faulting. The presence of numerous fault-related folds and fold-accommodation faults in this area demonstrates the close kinematic relationship between folding and faulting. Based on the topographic changes, a major hidden tear fault and a basement hidden back thrust have been suggested.**

Keywords- fold-accommodation fault; fault-related fold; Zagros orogenic belt; Sanandaj-Sirjan Zone (SSZ)

چهل و دومین گردهمایی (همایش) ملی

علــوم زمیـــن

The 42nd National
Geosciences Congress

www.geoconf.ir

ISC

1. Introduction

Folds and faults, as representatives of separate ductile and brittle deformations, were previously thought to only form in completely different tectonic settings [1–4]. However, these common structures can also develop simultaneously in a geodynamic environment as a result of kinematically related tectonic processes [5–8]. The fold-accommodation faults [7, 9, 10] and the fault-related folds [5, 11–13] are the two broad categories of structures that illustrate the complete kinematic relationship between faults and folds. The fault-related folds in the southern part of the Zagros hinterland have been explained before [14]. The present study aims to investigate the fold-accommodation faults.

2. Geological setting

The Zagros has always been studied from a variety of viewpoints [15–18]. The Zagros formed as a result of the subduction of the Neo-Tethyan oceanic lithosphere from the Jurassic to the Cenozoic and the subsequent collision of the Arabian plate with the Iranian plate in Cenozoic [19–24] (Fig. 1). This collisional belt is approximately 2000 km long and comprises some parallel subdivisions [25–30]. The study area is located in the Zagros Hinterland Fold-and-Thrust Belts.
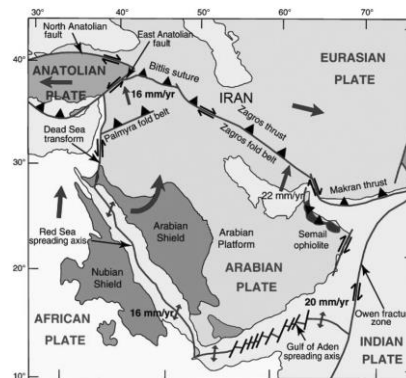

Figure 1. A simplified map showing the situation of the Zagros. In this figure, plate boundaries, approximate plate convergence vectors, and some key geologic features are mapped for a better understanding of the tectonic situation of the region [31].

2.1. Exposed stratigraphic units of the study area and its surroundings

All of the exposed stratigraphic units of the study area (Figs. 2, 3) are explained below. The Upper Devonian gray metaterrigenous unit is one of the oldest exposed stratigraphic units in the study area, outcropped south of the Sorkhouy Mountain (Fig. 3). This unit is overlain by the Visean quartz arenite unit, which is at the base of the dark gray Carboniferous well-bedded limestones. Light to dark gray Permian well-bedded limestone is the next unit, with the brownish-red Lower Permian sandstone and shale at the base. The Lower Triassic thinly-bedded marl and limestone are the younger exposed units in this area. All of the mentioned units in the study area are influenced by low-grade metamorphism. The Upper Oligocene-Lower Miocene thickly-bedded to massive limestone overlies the Triassic units in the northwest of the study area with angular unconformity [14]. There is a horizontal conglomerate unit on the sub-vertical layers of the Carboniferous limestones in the southernmost part of the Dareh-Nar valley (Fig. 4A). This unit has not been reported in the previous maps [32–34] and articles [14, 30] of the study area. The particles of this unit are not well sorted (Fig. 4B), but the rock is very well cemented. The granules, pebbles, cobbles, and boulders of this unit are angular and mostly composed of the limestones of the Carboniferous and Permian periods, as well as sandstone, and quartz arenites of the Visean.
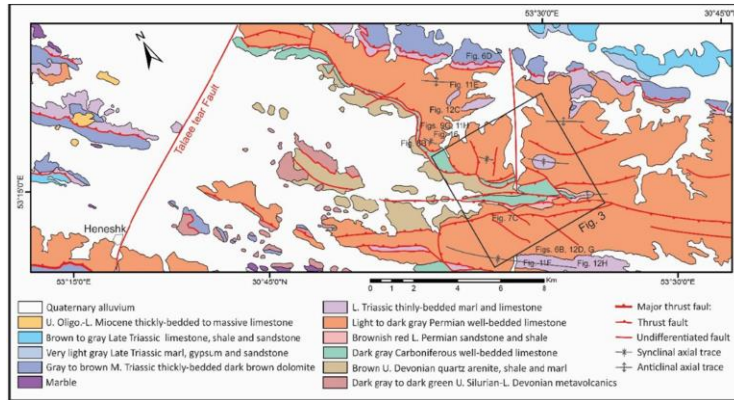
چهل و دومین گردهمایی (همایش) ملی
علــوم زمیــن
The 42nd National
Geosciences Congress

www.geoconf.ir

ISC

Figure 2. The geological map of the study area.

3. Data and method

In order to investigate the structural architecture and particularly the faults and folds relations, the vertical aerial photographs at 1:50,000 scale and the Landsat 8 satellite images were considered. Utilizing this data, map-scale structures have been mapped (Figs. 2, 3). While large-scale structures form the structural framework of the ZHFTB, mesoscopic ones are very valuable because it has been accepted as Pumpelly's rule that the characteristics of map-scale architecture can be cleared up by surveying minor structures [35]. Therefore, intensive field campaigns were conducted in the various parts of the study area, and outcrop-scale structures, including mesoscopic folds, different kinds of mesoscopic faults, and shear zones, were studied. Aerial photography becomes significantly more effective when a stereoscope is used in the field to gain a better understanding of field relationships. Using this advantage, it became clear that the mean elevation of the Faryadoun Mountain and the Dareh-Nar valley has changed significantly. As a result, approximately six kilometers of NNE-SSW topographic profiles have been constructed in this area to study this topographic contrast.
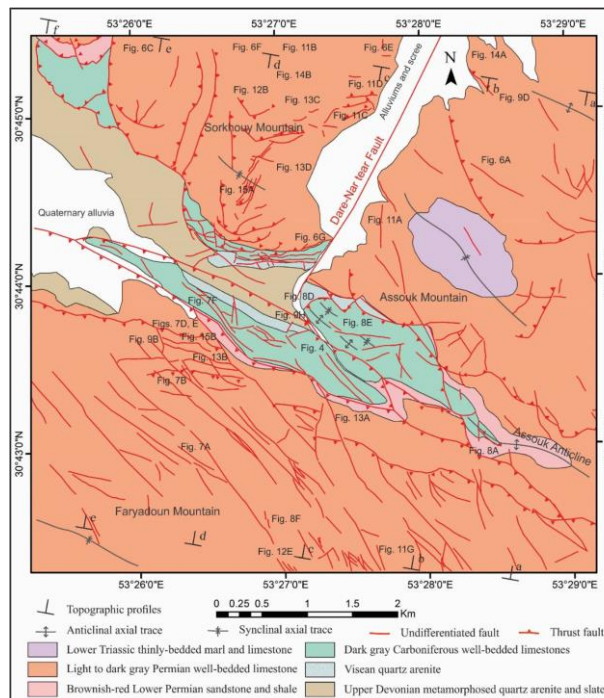

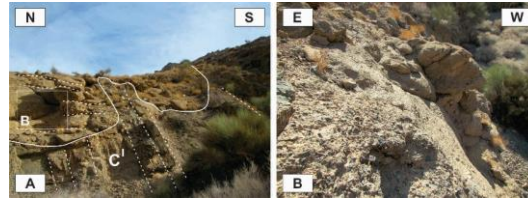Fig. 3. The geological map of the Faryadoun and Dare-Nar area.

Fig. 4. A horizontal conglomerate unit on the sub-vertical layers of the Carboniferous well-bedded limestones in the southernmost part of Dareh-Nar valley.

4. Results

4.1. Structural characteristics of the study area

The tectonic structures in the area occurred on a wide range of scales. The characteristics of map-scale structural architecture are formed by the large-scale structures (Fig. 3). The structures that play the most important roles in the tectonic framework of the study area are the various kinds of faults, folds, and shear zones. In this study, the faults were recognized from topographic variations, strike separations, and the bedding attitudes or lithological characteristics observed during the field investigations, as well as from aerial photographs stereoscopy, satellite image interpretations, and topographic profile considerations. Vertical aerial photographs have been used as a basis for field mapping, plotting dips, strikes, attitudes of faults, and contacts. The characteristics of the map-scale structures can be cleared up by surveying more reachable abundant outcrop-scale structures. The surface exposures of the faults are more frequently observed in the more competent units. The faults are one of the most abundant structures in the Dareh-Nar and Faryadoun areas (Figs. 2, 3, 5). There is a big difference in the scale of the faults in the range of map-scale to outcrop-scale (Fig. 5).
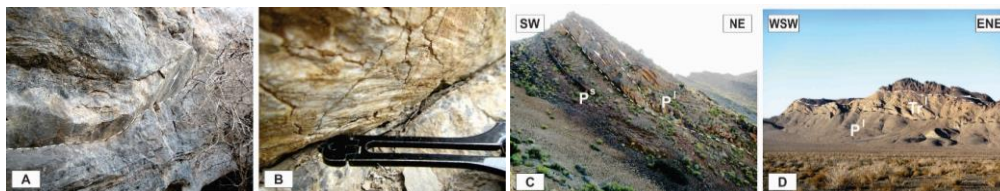

Fig. 5. Some field photographs of two examples of faults' planes and slickenlines (A and B), and the map-scale thrusts and reverse faults (C and D) of the study area. The compass needle is 55 mm long and toward N.

4.2. Map-scale faults

It seems that the Dare-Nar valley has been formed due to an NNE–SSW tear fault. The change in the attitude of the layers on both sides of the Dare-Nar valley and the sharp scarp on the northwestern side of the valley confirm the existence of this tear fault, which is named here the Dare-Nar tear fault (Figs. 2, 3). The two most notable types of map-scale faults are thrusts (or reverse faults) and strike-slip faults, which are generally WNW–ESE and NW–SE striking, respectively. The strike-slip faults (Fig. 6A) have been more developed in the south of the study area, while the thrust and reverse faults (Figs. 5, 7B–D) have been more developed in the north of the study area. The general tectonic vergence of the region is to the SW. Despite the existence of several considerable back thrusts (i.e., SW dipping), most of the thrusts in the area are NE dipping, which brought the different units from NE to SW. The bends in the faults' surfaces resulted in fat-ramp-fat geometries, and these geometries, in turn, caused folding in the hanging wall blocks (fault-bend folds; Fig. 5C). There is also a map-scale into-anticline thrust in the Assouk anticline (Fig. 7A). The strike line of this steeply dipping reverse fault is NW–SE, which is parallel to the axial plane of the Assouk anticline and its dip is toward the NE. Even though the strikes of most of the strike-slip faults are N40°W, there are some such faults with strikes ranging between N20°–70° W in the Faryadoun Mountain (Fig. 3). The strike-slip faults are vertical or semi-vertical and dextral, while the dip of most of the thrusts and reverse faults is 10°–40°.

چهل و دومین گردهمایی (همایش) ملی
علــوم زمیـــن
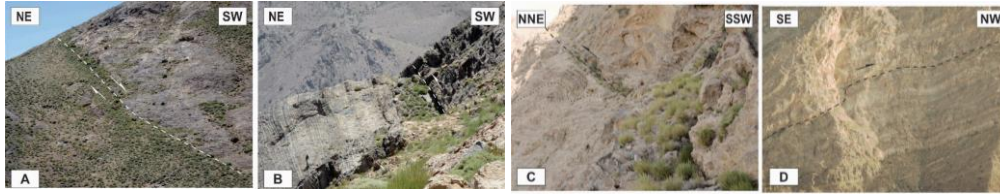The 42nd National
Geosciences Congress
www.geoconf.ir
ISC

Fig. 6. Annotated field photograph of a map-scale strike-slip fault (A) and a map-scale back thrust of the study area (B-D).
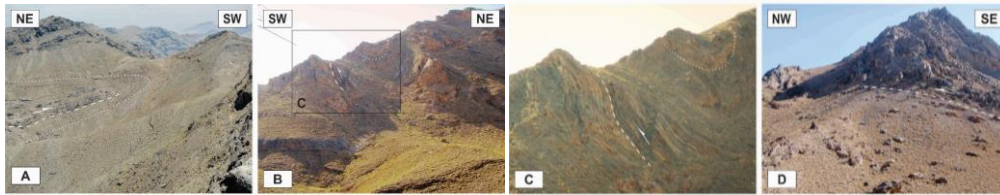

Fig. 7. A-D. Annotated field photographs of the several map-scale folds.

4.3. Topographic step

A considerable topographic step is also recognizable between the Faryadoun Mountain and its northern area. The average elevations in the north and south of this topographic step on the plotted profiles are 2010 and 2700 m, respectively (Fig. 8). This elevation contrast confirmed that there is a meaningful topographic step between the Faryadoun Mountain in the south and the Dareh-Nar valley in the north. The best explanation for the existence of this topographic step is the activity of a hidden basement SW-dipping thrust. Considering the overall tectonic vergence of the study area, which is to the SW, the NE verging basement fault is a back thrust. This inferred basement fault is named the Dareh-Bagh thrust.
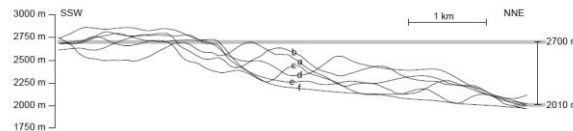

Fig. 8. Six topographic profiles have been constructed in the study area which show a significant change (about 700 m) in the mean elevation between the Faryadoun Mountain its northern area. See fig. 3 for the locations.

4.4. Map-scale folds

In the study area, there are several map-scale symmetric and asymmetric folds formed by the Devonian to Triassic rocks (Figs. 2, 3, 7). They have occurred in the hanging wall and footwall blocks of the map-scale faults in which their axes or hinges are parallel or semi-parallel to these faults' strike (NW–SE, Fig. 3). According to the diverse dips of their axial surfaces and the small plunge of their hinges, these macroscopic folds are horizontal inclined to upright and their profiles show that they are tight to open and even gentle folds. The Assouk anticline (Fig. 3) is the most prominent fold in the study area, which is a gently plunging, steeply inclined, tight fold in the north of the Faryadoun mountain. The Darreh-Bagh anticline and Darreh-Bagh syncline, which have been shown on the geological map of Kuh-e-Faryadon [34], have not been recognized in this study.

4.5. Outcrop-scale folds

There are lots of classes of mesoscopic folds at different scales with small wavelengths in the range of 0.02–10 m. These mesoscopic symmetric and asymmetric folds have chevron, concentric, and box profiles and mostly consist of thin-bedded limestones and dolostones. The axial planes are generally moderately to steeply dipping (50°–70°), although shallowly dipping (Fig. 9A) and vertical axial planes also occur. Despite the existence of

different folds such as upright to recumbent and horizontal to vertical folds, the horizontal inclined folds are the more abundant (Figs. 9B, C). The interlimb angles vary greatly, but most of the outcrop-scale folds in the study area are too tight to open. They are located in the tilted layers, the limbs of the map-scale folds, and even in the brittle-ductile shear zones associated with small-scale faults in these zones (Figs. 9D, E). The trends of the folds' axes, which are located on the tilted layers and the limbs of the map-scale folds, are mostly similar to the map-scale folds, which are semi-parallel to the strike of most of the thrust faults of the area (Fig. 10A); while the trends of the folds that are located in the brittle-ductile shear zones depend on the attitude and the sense of movement of the shear zones, the trends of their axes are generally normal to the displacement vectors of the shear zones. In addition, there are some outcrop-scale detachment (decollement) folds (Fig. 9F) which developed when displacements along bedding-parallel detachment faults (with no ramp) have been transferred into the folding of the hanging wall blocks.
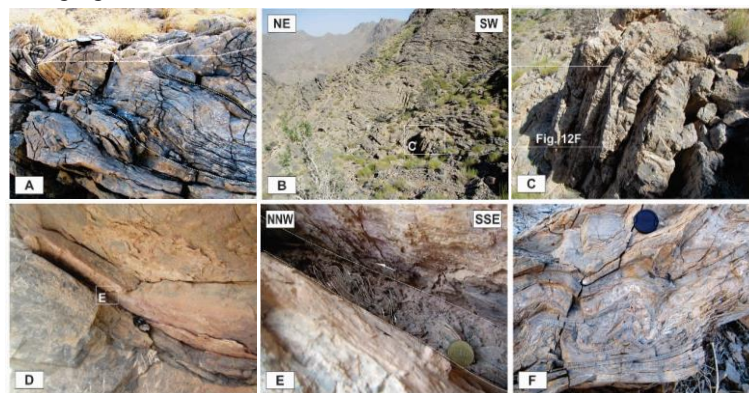

Fig. 9. Annotated field photographs of the various kinds of the outcrop-scale folds in the different parts of the study area.

4.6. Outcrop-scale faults

There are different types of mesoscopic faults in the study area, such as various types of thrust (Figs. 10B, 11A–F, 12A–H), strike-slip (Fig. 13A, B), and normal faults (Fig. 13C, D). The outcrop-scale thrusts occurred as the cause and/or result of the mesoscopic folds or without any obvious relationship to them. As a result of the activity of these numerous outcrop scale thrusts, some typical mesoscopic duplex structures formed (Fig. 11F). The hinge zones and limbs of the observed symmetric and asymmetric outcrop-scale folds have usually been dissected by mesoscopic thrust faults. The strikes of these thrust faults are mostly parallel to the hinge zones of the mesoscopic folds. These cm-displacement thrust faults cut only a few layers. As well as the different types of mesoscopic fault-related folds, especially the various kinds of outcrop-scale fold-accommodation faults [7], such as the back thrusts (Fig. 12A, B), the forelimb thrusts (Fig. 12C), the forelimb space-accommodation thrusts (Fig. 12D), the hinge wedge thrusts (Fig. 12E), the limb wedge thrusts (Fig. 12F), the out-of-syncline thrusts (Fig. 12G) and the into-anticline thrusts (Fig. 12H) are the common structures in the study area. There are a lot of slickensides on the contact surfaces of the tilted layers in the limbs of the map-scale folds (Fig. 14). The slickenlines are generally perpendicular to the folds' axes. Similar to the map-scale strike-slip faults, the outcrop-scale ones (Figs. 13A, B) are vertical to semi-vertical, often dextral, and more dominant in the southern parts of the study area (i.e., Faryadoun Mountain), with strikes that are generally similar to the other aforementioned faults (NW–SE). Outcrop-scale normal faults are the other obvious structures in the study area. The prevailing dips of these m-displacement faults are 55°–65°. Their attitudes vary considerably, but the E-striking ones are more frequent.
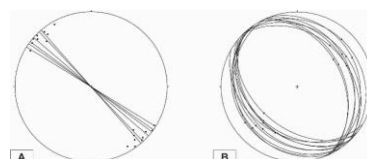

Fig. 10. A. Stereographic projection from the lower hemisphere showing the trend of map-scale folds (lines; No.=7) and the attitudes of the axes of the outcrop-scale folds (points; No.=19). B. Stereographic projection from the lower hemisphere showing the attitudes of the outcrop-scale thrusts (No.=18).
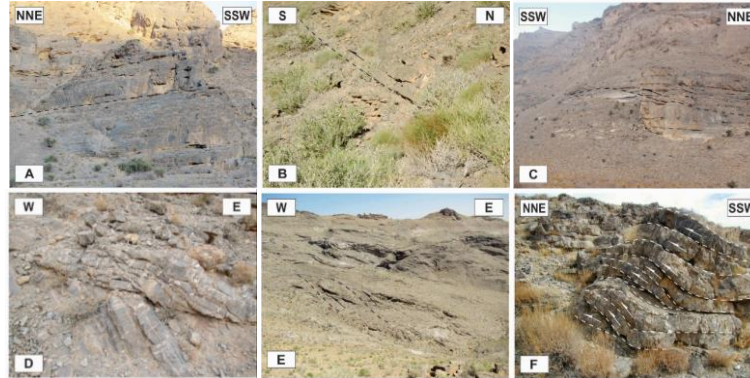
چهل و دومین گردهمایی (همایش) ملی
علـوم زمیـن
The 42nd National
Geosciences Congress
www.geoconf.ir
ISC

Fig. 11. Annotated field photograph of the examples of the outcrop-scale thrust faults and duplex structures.

4.7. Layer-parallel ductile shear zones

In the Sorkhouy, Faryadoun, and Assouk mountains, there are many layer-parallel narrow ductile shear zones. They are mostly NNW-SSE striking, ENE gently dipping in the Sorkhouy and Assouk mountains (Fig. 15A), and NW–SE striking, SE dipping in the Faryadoun mountains (Fig. 15B). These shear zones have been formed in the less competent layers and have facilitated the shearing of the layers. They consist of layers of parallel calcite mylonitic foliation. Deformed chert nodules are plentiful in these shear zones (Fig. 15B). These less competent layers have been eroded more than the other layers (Fig. 15).
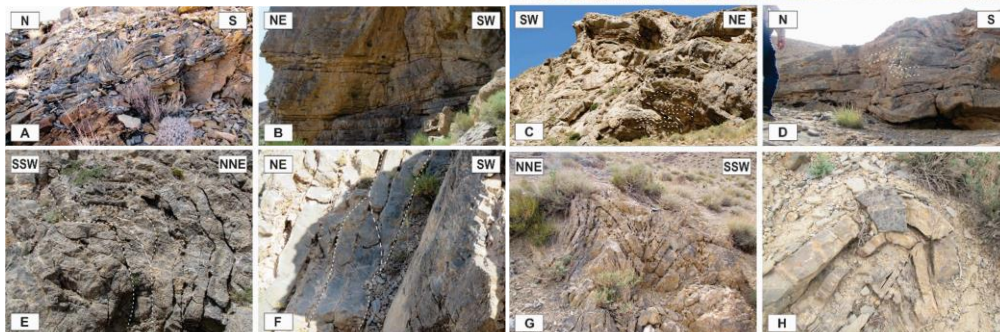

Fig. 12. Annotated field photograph of some of the outcrop-scale fold-accommodation faults. A and B. Back thrusts. C. A Forelimb thrust. D. A forelimb space-accommodation thrust. E. A hinge wedge thrust. F. A limb wedge thrust. G. An out-of-syncline thrust. H. An into-anticline thrust.
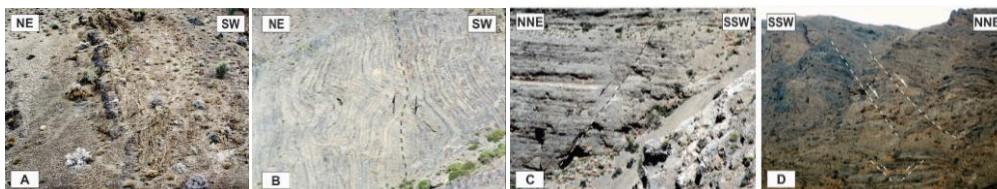

Fig. 13. Annotated field photograph of the outcrop-scale strike-slip (A and B) and normal (C and D) faults.
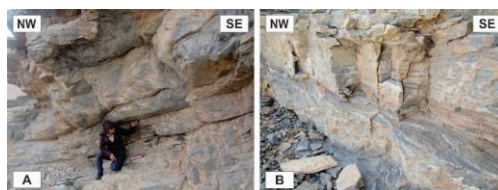

Fig. 14. The slickensides on the contacts' surfaces of the tilted layers in the limbs of the map-scale folds.
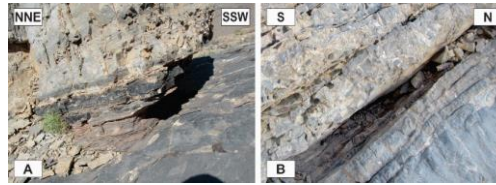
Fig. 15. The Layer-parallel ductile shear zones.

5. Discussion

The SSZ is the inner part of the Zagros collisional zone which is deformed severely [39]. It has been developed as a consequence of the subduction of the Neotethyan oceanic plate under the Central Iranian microplate in the Jurassic to Cenozoic and the subsequent collision between this and the Arabian plate in the middle of the Cenozoic [20, 39]. The SSZ has been divided into the southwestern metamorphic zone (i.e., SSMB) and the northeastern metasedimentary belt (i.e., ZHFTB) [14, 30]. Almost all of the study area, which is the south-central part of the ZHFTB, is affected by low-grade metamorphism, except the units younger than the Early Eocene. According to the age dating results of the SSZ [40], the metamorphism of the area is considered to be older than the Eocene. There is at least one sinistral top-to-the NW shearing [30, 35, 36, 38] which is older than Neogene [40]. This sinistral top-to-the NW deformation is not restricted to this area [15, 41]. The fabric of Heneshk (Kowlikosh) shear zones (Fig. 12 in [42]) and the Neyriz area (Fig. 3 in [43]), also, indicate the occurrence of sinistral deformation in the different parts of SSMB. In the ZHFTB, the two architectural structures are faults and folds. In addition to the exposed macroscopic faults and folds, which have been presented on the maps (Figs. 2, 3), two hidden faults have been introduced in this study: the Dare-Nar tear fault along the linear Dare-Nar valley (Figs. 2, 3), and the Dare-Bagh back thrust, which resulted in a prominent topographic step in the north of the Faryadoun mountain. The effects of hidden basement faults on the surface topography have been reported in many other areas, such as the Darang and Surmeh anticlines [44]. The cause of the existence of the Dare-Nar valley seems to be a NE-SW striking tear fault (i.e., the Dare-Nar tear fault), similar to the Talaee tear fault [14]. The relationships of the faults and folds in the outcrop-scale fault-bend folds and fold accommodation faults are more obvious than their association in the map-scale structures. The map-scale thrust faults on the limbs of the map-scale folds, however, suggest that these folds could develop as thrust-related folds [45]. Thus, the fault-related folds were observed at different scales and in the various types of fault-bend folds and asymmetric detachment folds. Several incompetent layers, such as the Upper Devonian metaterrigenous unit, the Lower Permian sandstone and shale, and the Lower Triassic thinly-bedded marl and limestone, acted as the detachment surfaces and facilitated occurrences of the thrust systems, detachment folds, and layer parallel shear zones. There is no evidence of a map-scale roof thrust, so the thrust systems are mostly imbricate fans. This is in contrast with the idea of Sarkarinejad and Ghanbarian [14], which suggested that the structural architecture of the area is characterized by several duplex structures. Several successive map-scale foreland dipping horses, however, occurred in the center of the study area and north of the Faryadoun mountain (Fig. 3). Therefore, the thrust faults play the most determining roles in the structural architecture of the study area, and many other structures, such as folds, have occurred as a result of their development. Sarkarinejad and Ghanbarian [14] emphasized the determining role of the map-scale forethrusts, too. The map-scale back thrusts of the study area (Fig. 7C–D), which are very significant structures in the area (Fig. 3), can occur due to the fat-ramp geometry of a main underground fore thrust, the occurrence of pop-up structures, and the steepening of the underlying foreland-dipping duplexes (due to ongoing shortening of the area), which bend the flat thrusts to the SW-dipping thrust. These back thrusts can also be the continuation of the Dareh-Bagh basement back thrust, which caused the main topographic contrast in the vicinity of the main exposed back thrusts of the study area (i.e., the north of the Faryadoun mountain; Fig. 3). Within the folds of the study area, there are different kinds of faults that have developed due to folding processes. Forelimb thrusts, forelimb space-accommodation thrusts, back thrusts, out-of-syncline and into-anticline thrusts, wedge thrusts including hinge wedges and limb wedges thrusts are the diverse modes of the fold accommodation faults of the study area. Nevertheless, the geometric and kinematic relationship between thrust faults and folds are scale-invariant, as discussed by Sarkarinejad and

Ghanbarian [14]. The existence of many slickensides between tilted layers in the macroscopic folds' limbs suggests that there are layer parallel slips that developed during flexural slip folding. The Upper Oligocene–Lower Miocene reefal limestones are involved in younger than the earliest Miocene thrusting. Some dextral strike-slip faults have cut the northern parts of Faryadoun Mountain (Fig. 3). There is no apparent kinematic relationship between the strike-slip faults and folds. Therefore, there must be at least two major events, (1) a ductile one older than the Eocene, which is accompanied by metamorphism, and (2) a semi-brittle deformation younger than the earliest Miocene. The latter is represented by folding, thrusting, and strike-slip faulting. The folding and faulting in this event are interrelated, as shown by the existence of various fault-related folds and fold-related faults in the area. This kinematic association suggests that this second deformation event is not completely brittle.

6. Conclusion

The structural analysis of this part of the ZHFTB was based on aerial photographs stereoscopy, satellite images interpretations, consideration of the major topographic changes, and field investigations. The results of this research revealed that there must be at least two main deformation phases, (1) a ductile event, which is older than Eocene and accompanied by metamorphism, and (2) a semi-brittle deformation phase that is younger than the earliest Miocene and is represented by thrusting, folding, and strike-slip faulting. The abundant fault-related folds and fold-accommodation faults of the study area reveal the close connection between folding and faulting in this region. A basement hidden back thrust and a major hidden tear fault has been introduced in this study based on the surface topographic changes. The basement hidden back thrust may be the cause of the map-scale back thrusts and other structures in the north of Faryadoun Mountain

References

[1] Crittenden, M. D. Jr. 1974. Regional extent and age of thrusts near Rockport Reservoir and relation to possible exploration targets in Northern Utah. AAPG Bull. 58, 2428–2435.
[2] Geiser, P., Engelder, T. 1982. Distribution of layer-parallel shortening fabrics in Appalachian Foreland of New York and Pennsylvania: Evidence for two non-coaxial phases of alleghany orogeny. AAPG Bull. 66, 1168–1168.
[3] van der Pluijm, B. A. 1987. Timing and spatial distribution of deformation in the Newfoundland Appalachians: A "multi-stage collision" history. Tectonophysics 135, 15–24. https:// doi. org/ 10. 1016/ 0040- 1951(87) 90148-X.
[4] Hibbard, J., Hall, S. 1993. Early Acadian sinistral shear in north-central Maine, USA. J. Geol. Soc. 150, 815–818.
[5] Jamison, W. R. 1987. Geometric analysis of fold development in overthrust terranes. J. Struct. Geol. 9, 207–219.
[6] Mitra, S. 1990. Fault-propagation folds: Geometry, kinematic evolution, and hydrocarbon traps. AAPG Bull. 74, 921–945.
[7] Mitra, S. 2002. Fold-accommodation faults. AAPG Bull. 86, 671–693.
[8] Suppe, J., Connors, C. D. & Zhang, Y. 2004. Shear fault-bend folding. In: K. R. McClay, 2004, Thrust tectonics and hydrocarbon systems: AAPG Memoir 82, 303–323.
[9] Li, T. et al. 2021. The 2019 Mw 58 Changning, China earthquake: A cascade rupture of fold-accommodation faults induced by fluid injection. Tectonophysics 801, 228721.
[10] Tavani, S. et al. 2015. A review of deformation pattern templates in foreland basin systems and fold-and-thrust belts: Implications for the state of stress in the frontal regions of thrust wedges. Earth Sci. Rev. 141, 82–104.
[11] Machuca, S., García-Delgado, H., Velandia, F. 2021. Studying active fault-related folding on tectonically inverted orogens: A case study at the Yariguíes Range in the Colombian Northern Andes. Geomorphology 375, 107515.
[12] Mathew, G., Singhvi, A. K., Karanth, R. V. 2006. Luminescence chronometry and geomorphic evidence of active fold growth along the Kachchh Mainland Fault (KMF), Kachchh, India: Seismotectonic implications. Tectonophysics 422, 71–87.
[13] Hamdon, A. N., Znad, R. K. 2021. An emerging fault related fold (Mahad Anticline) and its morphotectonic interpretations in Northern Iraq. Iraqi J. Sci. 62, 1550–1561.
[14] Sarkarinejad, K., Ghanbarian, M. A. 2014. The Zagros hinterland fold-and-thrust belt in-sequence thrusting, Iran. J. Asian Earth Sci. 85, 66–79.
[15] Ghanbarian, M. A., Yassaghi, A., Derakhshani, R. 2021. Detecting a sinistral transpressional deformation belt in the Zagros. Geosciences 11, 226.
[16] Ghanbarian, M. A., Derakhshani, R. 2022. Systematic Variations in the Deformation Intensity in the Zagros Hinterland Fold-and-Thrust Belt, Iran. Z. Deutschen Gesellschaft Geowissenschaften. 173 (1).
[17] Stöcklin, J. 1974. The Geology of Continental Margins 873–887, Springer.
[18] Talbot, C., Alavi, M. 1996. The past of a future syntaxis across the Zagros. Geol. Soc. Lond. Spec. Publ. 100, 89–109.
[19] Berberian, M., King, G. 1981. Towards a paleogeography and tectonic evolution of Iran. Can. J. Earth Sci. 18, 210–265.
[20] Mohajjel, M., Fergusson, C. 2014. Jurassic to Cenozoic tectonics of the Zagros Orogen in NW Iran. Int. Geol. Rev. 56, 263–287.
[21] Derakhshani, R., Farhoudi, 2005. G. Existence of the Oman Line in the Empty Quarter of Saudi Arabia and its continuation in the Red Sea. J. Appl. Sci. 5, 745–752.

[22] Mehrabi, A., Dastanpour, M., Radfar, S., Vaziri, M., Derakhshani, R. 2015. Detection of fault lineaments of the Zagros fold-thrust belt based on Landsat imagery interpretation and their relationship with Hormuz series salt dome locations using GIS analysis. Geosciences 24, 17–32.

[23] Rahnamarad, J., Farhoudi, G., Ghorbani, H., Habibimood, S., Derakhshani, R. 2009. Pierced salt domes in the Persian Gulf and in the Zagros mountain ranges. Iran. J. Earth Sci. 1, 57–72.

[24] Alavi, M. 2004. Regional stratigraphy of the Zagros fold-thrust belt of Iran and its proforeland evolution. Am. J. Sci. 304, 1–20.

[25] Bigi, S., Carminati, E., Aldega, L., Trippetta, F., Kavoosi, M. A. 2018. Zagros fold and thrust belt in the Fars province (Iran) I: Control of thickness/rheology of sediments and pre-thrusting tectonics on structural style and shortening. Mar. Pet. Geol. 91, 211–224.

[26] Mouthereau, F., Lacombe, O. & Vergés, J. 2012. Building the Zagros collisional orogen: Timing, strain distribution and the dynamics of Arabia/Eurasia plate convergence. Tectonophysics 532, 27–60.

[27] Carminati, E., Aldega, L., Bigi, S., Minelli, G., Shaban, A. 2016. Not so simple "simply-folded Zagros": The role of pre-collisional extensional faulting, salt tectonics and multi-stage thrusting in the Sarvestan transfer zone (Fars, Iran). Tectonophysics 671, 235–248.

[28] Casciello, E. et al. 2009. Fold patterns and multilayer rheology of the Lurestan, Zagros folded belt (Iran). J. Geol. Soc. 166, 947–959.

[29] Stocklin, J. 1968. Structural history and tectonics of Iran: A review. AAPG Bull. 52, 1229–1258.

[30] Ghanbarian, M. A., Yassaghi, A. 2020. Structural and microstructural analyses of the deformation in the Faryadoun region, NE of the Zagros orogenic belt: Evidence for the occurrence of the sinistral shear. Geosciences 30, 243–252.

[31] Stern, R. J., Johnson, P. 2010. Continental lithosphere of the Arabian Plate: A geologic, petrologic, and geophysical synthesis. Earth Sci. Rev. 101, 29–67.

[32] Shahidi, A., Taraz, H., Zamani, P., Alavi, M., PartoAzar, H. 1999. Geological map of the Dehbid area. GSI Iran Scale 1, 100000.

[33] Soheyli, M. et al. 1990. Geological Map of the Eghlid Area. Geological Survey of Iran, Tehran, Iran, Scale: 1:250,000.

[34] Haftlang, R. et al. 2013. Geological map of Kuh-e-Faryadon. Sheet No. 6651II NE. Scale: :25000. GSI, Tehran, Iran.

[35] Ghanbarian, M. A. 2014. Kinematic Analysis of the Tectonic Structures in the Hinterland of the Zagros Orogenic Belt, Iran PhD thesis. Shiraz University.

[36] Ghanbarian, M. A., Sarkarinejad, K. 2014. Evidences of sinistral flow in the Zagros inclined transpression, Iran. The 2nd national symposium on tectonics of Iran, Geological survey of Iran, Tehran, Iran.

[37] Ghanbarian, M. A., Yassaghi, A., Sadeghi mazidi, M. in 2nd TRIGGER International Conference, Trans-disciplinary Research on Iranian Geology, Geodynamics, Earthquakes and Resources (Tehran, Iran, 2018).

[38] Sadeghi Mazidi, M. 2019. Paleo Stress Analysis of the Zagros Hinterland Fold-and-Thrust Belt in Bavanat to Shurjestan. MS thesis. Shiraz Uni.

[39] Mohajjel, M., Fergusson, C., Sahandi, M. 2003. Cretaceous-Tertiary convergence and continental collision, Sanandaj-Sirjan zone, western Iran. J. Asian Earth Sci. 21, 397–412.

[40] Shakerardakani, F. et al. 2015. Panafrican basement and Mesozoic gabbro in the Zagros orogenic belt in the Dorud-Azna region (NW Iran): Laser-ablation ICP–MS zircon ages and geochemistry. Tectonophysics 647, 146–171.

[41] Sarkarinejad, K., Partabian, A., Faghih, A. 2013. Variations in the kinematics of deformation along the Zagros inclined transpression zone, Iran: Implications for defining a curved inclined transpression zone. J. Struct. Geol. 48, 126–136.

[42] Sarkarinejad, K., Azizi, A. 2008. Slip partitioning and inclined dextral transpression along the Zagros Thrust System, Iran. J. Struct. Geol. 30, 116–136.

[43] Sarkarinejad, K., Faghih, A., Grasemann, B. 2008. Transpressional deformations within the Sanandaj-Sirjan metamorphic belt (Zagros mountains, Iran). J. Struct. Geol. 30, 818–826.

[44] Mouthereau, F., Lacombe, O. & Meyer, B. 2006. The Zagros folded belt (Fars, Iran): Constraints from topography and critical wedge modelling. Geophys. J. Int. 165, 336–356.

[45] Konon, A. 2006. Buckle folding in the Kielce Unit, Holy Cross Mountains, central Poland. Acta Geol. Pol. 56, 375–405.